

8232-2/43846
C. 4

845
AUG

1-5.1

SAND74-8031
Unlimited Release

Performance Calculations for a High Temperature Solar Energy Collection System

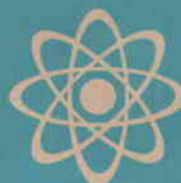
C. M. Leonard, Jr.

Prepared by Sandia Laboratories, Albuquerque, New Mexico 87115 and Livermore, California 94550 for the United States Atomic Energy Commission under Contract AT (29-1)-789

Printed January 1975



Sandia Laboratories
energy report



Cat No: 21.3001

Issued by Sandia Laboratories, operated for the United States Atomic Energy Commission by Sandia Corporation.

NOTICE

This report was prepared as an account of work sponsored by the United States Government. Neither the United States nor the United States Atomic Energy Commission, nor any of their employees, nor any of their contractors, subcontractors, or their employees, makes any warranty, express or implied, or assumes any legal liability or responsibility for the accuracy, completeness or usefulness of any information, apparatus, product or process disclosed, or represents that its use would not infringe privately owned rights.

SF 1004-DF(2-74)

SAND74-8031
Unlimited Release
Printed January 1975

PERFORMANCE CALCULATIONS FOR A HIGH TEMPERATURE
SOLAR ENERGY COLLECTION SYSTEM

C. M. Leonard, Jr.
Command and Control Division 8365
Sandia Laboratories

ABSTRACT

A high-temperature, central receiver solar energy collection system is modeled with the DAZZLE computer program. Results for a large hypothetical system located near Albuquerque, New Mexico are given for clear weather on spring equinox, and summer and winter solstice days, and for a year of typical Albuquerque weather as described in the U. S. Climatic Atlas.

TABLE OF CONTENTS

	<u>Page</u>
Introduction	9
System Model Description	10
System Geometry and Deployment	10
Sun Direction	12
Solar Flux Reflected to the Cavity Receiver	12
Solar Flux Collected by the Cavity Receiver	13
System Performance	14
Appendix A--Calculating the Direction of the Sun	19
Appendix B--Calculating Incident Solar Flux	23
Appendix C--Determining Reflected Solar Flux	29
References	31

ILLUSTRATIONS

<u>Figure</u>		<u>Page</u>
1.	A Nominal 300-MW _t Point Focus Solar Energy Collection System	8
2.	Point Focus Solar Energy Collection System Geometry	10
3.	Power Collected Versus Time of Day for a Nominal 300-MW _t Point Focus Solar Energy Collection System	15
4.	Annual Collected Solar Energy Versus System Mirror Density	15
5.	Solar Energy Collected on the Summer Solstice Versus System Mirror Density	16
6.	Peak Solar Power Collected on the Summer Solstice Versus System Mirror Density	16
7.	Annual Collected Solar Energy Versus Mirror Density for Peak Power Limitations of 90, 80, and 70 Percent of the Maximum Available Power on the Summer Solstice	17
8.	Annual Collected Solar Energy Versus Mirror Density for Various Cavity Aperture Areas	18

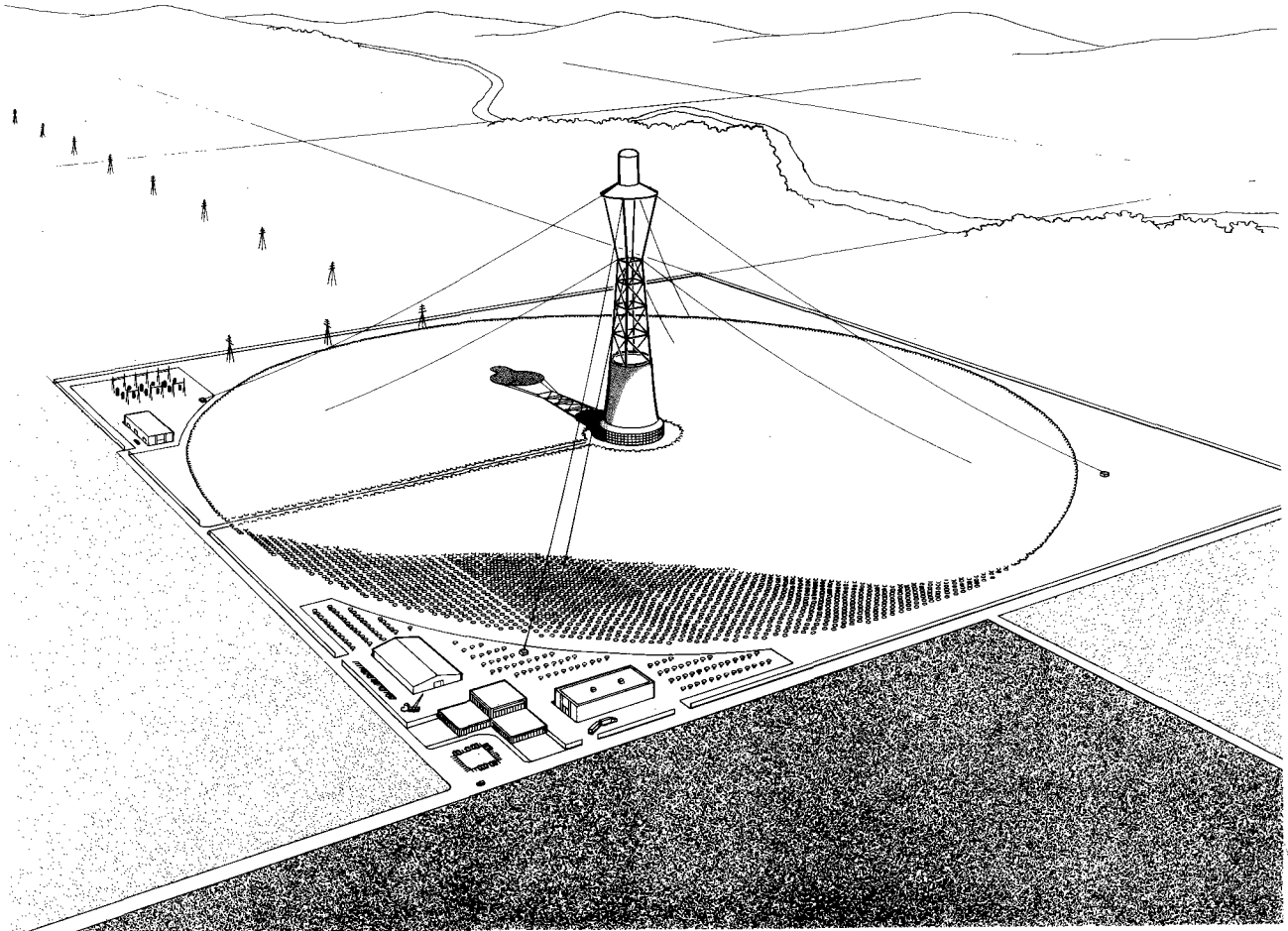


Figure 1. A Nominal 300 MW_t Point Focus Solar Energy Collection System

PERFORMANCE CALCULATIONS FOR A HIGH-TEMPERATURE SOLAR ENERGY COLLECTION SYSTEM

Introduction

The "energy crisis" that sent automobiles into gas lines and utility bills soaring also generated considerable interest in harnessing energy from the sun. Many different schemes are now being studied and developed--including heating and cooling of buildings, supplying heat for agricultural and industrial processes, and using solar energy to generate electricity.

As part of a research program directed toward using solar energy to generate electricity, * a method has been developed for calculating the performance of a large, high-temperature solar energy collection system. The 300-MW_t** collection system modeled, shown in Figure 1, is composed of a large array of individual mirrors that reflect sunlight to a receiver atop a central tower. The system calculations include earth-sun relationships, weather effects, shadowing of incident solar flux and blocking of reflected solar flux by adjacent mirrors in the mirror array, and operation of the system's central receiver. An allowance for thermal losses from system piping and heat exchangers is also included.

Modeling the operation of the point-focus solar collection system is divided into four tasks: describing the system geometry and deployment, determining the direction of the sun from the system site, determining the amount of solar flux reflected to the cavity receiver, and determining the amount of solar flux collected in the cavity receiver. These four tasks have been combined into a computer program, DAZZLE, which accepts a system description, location, weather data, and a specified period of system operation--hours, days, months, or a year--and calculates system performance.

This report describes how the necessary operations are performed in the DAZZLE program, and also presents daily and yearly totals of collected solar energy predicted by the program.

*This research is described in Reference 6.

**MW_t indicates megawatts-thermal; MW_e indicates megawatts-electric.

System Model Description

System Geometry and Deployment

As shown in Figure 2, the point-focus collection system modeled consists of a large circular array of individually-steered, nearly flat mirrors reflecting solar flux to the top of a centrally located tower, where it is collected in a cavity type receiver--a cylindrical cavity with a windowless aperture in its bottom. Reflected solar flux is admitted into the cavity receiver through the aperture and is absorbed over the cavity interior surface. This receiver configuration has the advantages of collecting the reflected flux over its large internal area at comparatively low flux density, of having radiation energy losses limited by the relatively small area of the cavity aperture, and of having a collection efficiency which tends to be greater than receivers which absorb energy at comparable flux densities on exterior surfaces. Use of a cavity receiver does require rather precise aiming and focusing of reflected solar flux so that it passes through the aperture and into the cavity interior.

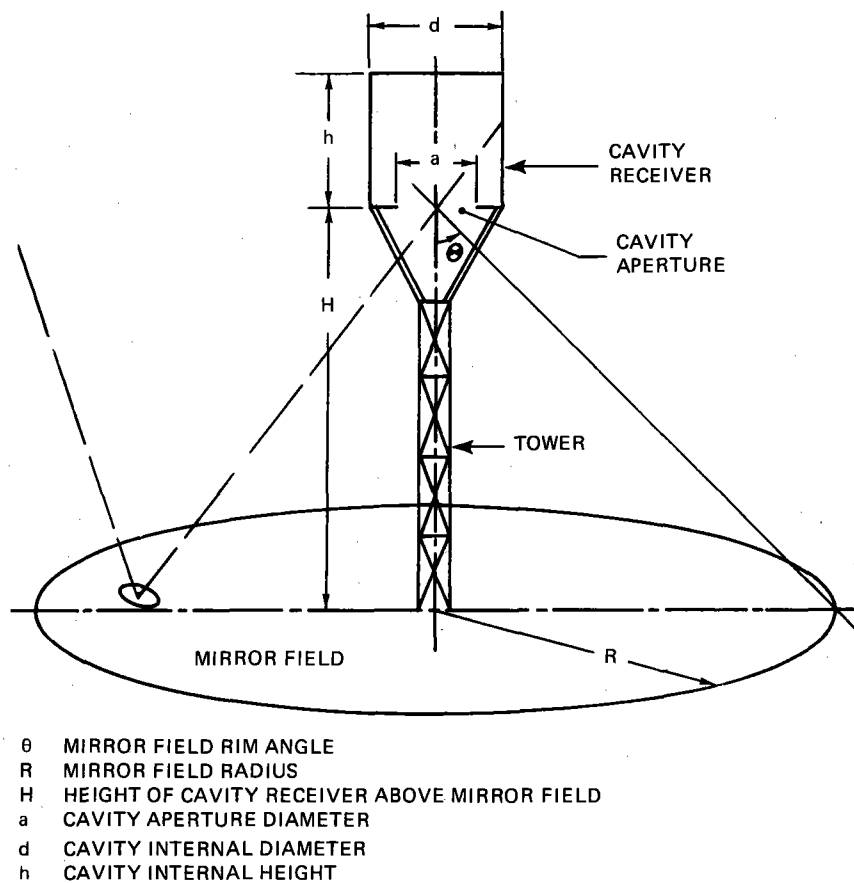


Figure 2. Point Focus Solar Energy Collection System Geometry

The point-focus collection system is characterized by the shape and dimensions of the mirror array or mirror field, the mirror deployment and mirror density, the height of the receiver above the mirror field, and the rim angle--the angle between the vertical axis of the cavity receiver and a line from the center of the cavity aperture to a mirror on the farthest edge of the mirror field. The characteristics of the nominal 300-MW_t point-focus system modeled in this study are given in Table I. Mirror density, defined as the total mirror area divided by the total ground area inside the mirror field perimeter, was adjusted from 0.9 to 0.1 in this study by changing the spacing between mirrors.

TABLE I
DESCRIPTION OF A NOMINAL 300 MW_t
POINT FOCUS SOLAR ENERGY COLLECTION SYSTEM

System Site Location	Albuquerque, New Mexico
Mirror Field Rim Angle	60°
Mirror Field Shape	Circular
Overall Mirror Density	0.5
Mirror Field Radius	520 m
Mirror Deployment	Uniform Spacing
Mirror Reflectivity	0.85
Receiver Height Above Mirrors	300 m
Receiver Type	Cylindrical Cavity
Cavity Aperture Diameter	18.1 m
Cavity Interior Height	21.5 m
Cavity Interior Diameter	20.0 m
Cavity Interior Temperature	811 K
Cavity Interior Emissivity	0.95

The individual mirrors are assumed to be round and deployed in a hexagonal pattern with equal spacing between adjacent mirrors over the entire field. This study did not examine the case of unequal spacing between mirrors or variable spacing over the field. (A separate study by J. D. Hankins indicates that the reflected solar energy from a given number of mirrors can be increased somewhat through the use of variable,

optimized spacing. *) It is also assumed that the mirrors are continually focusing--that is, as the sun position changes throughout the day, the surface of each mirror is continuously varied so that the beam from each mirror always passes through the cavity aperture.

Sun Direction

Modeling the operation of a point-focus system requires a description of the direction of the sun at each instant of time that the collected solar flux is calculated. A routine in the DAZZLE program accepts the system site latitude, the day of the year, and the time of day as input and returns the direction of the sun as a unit vector in the system site reference frame. For simplicity, the earth is assumed to move in a circular orbit about the sun instead of its true elliptical orbit. Details of this calculation are given in Appendix A.

Solar Flux Reflected to the Cavity Receiver

Modeling the operation of a point-focus system requires that the solar flux reflected from the mirror field be calculated, taking into account the effects of shadowing and blocking by adjacent mirrors. The solar flux reflected from the entire mirror field is found by dividing the mirror field into sections and calculating the solar flux reflected from each section. In this study, the mirror field was divided into 100 sections. (Dividing the field into 400 sections changed the results by less than 1/2 percent.) In each section, an individual round mirror was located at the center, surrounded by adjacent mirrors in a hexagonal pattern. Shadowing of incident solar flux and blocking of reflected solar flux by the adjacent mirrors was calculated and used to determine the solar flux reflected from the center mirror toward the cavity receiver. A description of the method used to calculate shadowing and blocking is given in Appendix C. The value of reflected and unblocked flux from the mirror at the center of a section was used as the flux value for each mirror in the section. Values of reflected flux calculated for each section were summed for the entire mirror field to give the total solar flux reflected toward the cavity receiver at a given time.

In this study, solar energy collected over a year was calculated by representing each month by an average day and summing the solar energy collected on each average day times number of days in the month it represents. The average day is taken as the fifteenth of the month and is defined

*See Reference 6, Section 6.2.

as having a daily total solar radiation on a horizontal surface (both direct radiation from the sun and diffuse radiation from clouds and sky) equal to the average daily total for that month given by the Climatic Atlas of the United States published by the U. S. Department of Commerce. Direct solar radiation from the sun was calculated using the solar constant (the extraterrestrial solar flux), the air mass traversed by the solar flux, and the atmospheric transmissivity. Diffuse solar radiation from the sky and clouds was calculated using the relationship developed by Liu and Jordan³ for diffuse solar radiation on a cloudy day. The total direct and diffuse solar radiation on the average day representing a month is made to agree with the average daily total solar radiation for that month given in the U. S. Climatic Atlas by artificially adjusting the value of the solar constant used in the calculation of direct solar radiation. The results of these calculations compare favorably with the relationship developed by the Aerospace Corporation in which direct solar radiation is related to the possible total solar radiation. The method is convenient for analyzing system performance at any of the many locations for which total insolation is available.

Solar Flux Collected by the Cavity Receiver

Operation of the cavity receiver is based on a two-zone radiation model¹ in which convection and conduction losses are assumed to be negligible. Cavity efficiency is given by:

$$\eta = \frac{\epsilon \left(1 - \frac{\sigma T^4}{C Q_R} \right)}{\epsilon + (1 - \epsilon)\theta}$$

η = cavity efficiency

ϵ = cavity internal emissivity

T = cavity internal temperature

C = system concentration ratio

Q_R = reflected solar flux per unit mirror area

θ = aperture area/cavity internal area

σ = Stefan-Boltzmann constant

The cavity efficiency was calculated for each time interval--20 minutes in this study--to determine the power collected by the cavity. The power available in the steam for the turbine-generator is the power collected in the cavity reduced by a small amount (0.5 percent of maximum power) to account for heat transfer losses in the heat transfer system and the steam generator.

System Performance

The power collected versus time of day for the nominal 300-MW_t system is shown in Figure 3 for clear weather on a summer solstice day, a spring equinox day, and a winter solstice day. Because of the changing declination of the sun and varying atmospheric transmissivity, the maximum power collected is over 300 MW_t in the spring and summer and lower than 300 MW_t in the winter.

The annual collected solar energy in thermal gigawatt-hours (GWh_t) is shown in Figure 4 as a function of mirror density. At the high values of mirror density, shadowing and blocking greatly reduce the effectiveness of added mirror area. At low values of mirror density, the effects of shadowing and blocking by adjacent mirrors are minimal and collected energy tends to be proportional to total mirror area (diminished, of course, by cavity energy losses).

Solar energy collected on a clear summer solstice day by the nominal system with a range of mirror densities is shown in Figure 5. The maximum power level for collected solar energy on a clear summer solstice day is shown in Figure 6.

The maximum power level of a point focus system varies throughout each day, and the maximum daily power level varies throughout the year. For economic considerations, it is of interest to determine the amount of solar energy collected annually by a system which has some upper limit (i. e., clipping level) on the power it can collect or use. This would correspond, for example, to a solar energy collection system which has essentially no energy storage capability and delivers energy directly to a turbine-generator which is rated at less than the maximum power available to the collection system. The annual collected solar energy would then be the energy that could be used by the turbine-generator. Figure 7 shows the annual collected solar energy versus system mirror density for limitations on collected power level of 90, 80, and 70 percent of the peak level of collectible power on the summer solstice. The values shown in Figure 7 are found by calculating the annual excess energy and subtracting this from the annual energy values shown in Figure 4. These values are conservative limits because the excess energy was calculated as though the excess power levels occurred around noon and always in clear weather. This technique results in the maximum amount of power being declared excess because in reality there would be times when hazy or cloudy weather prevailed at noon, resulting in somewhat lower levels of annual excess energy and higher levels of annual collected energy with a given maximum power limitation.

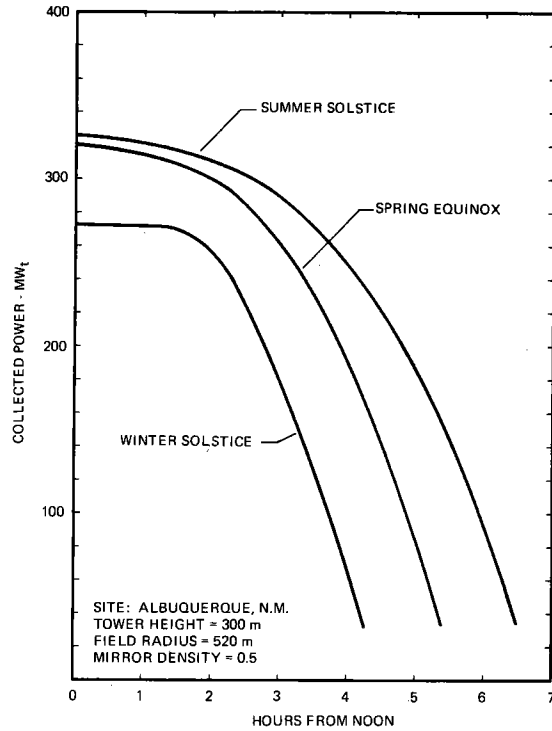


Figure 3. Power Collected Versus Time of Day for a Nominal 300 MW_t Point Focus Solar Energy Collection System

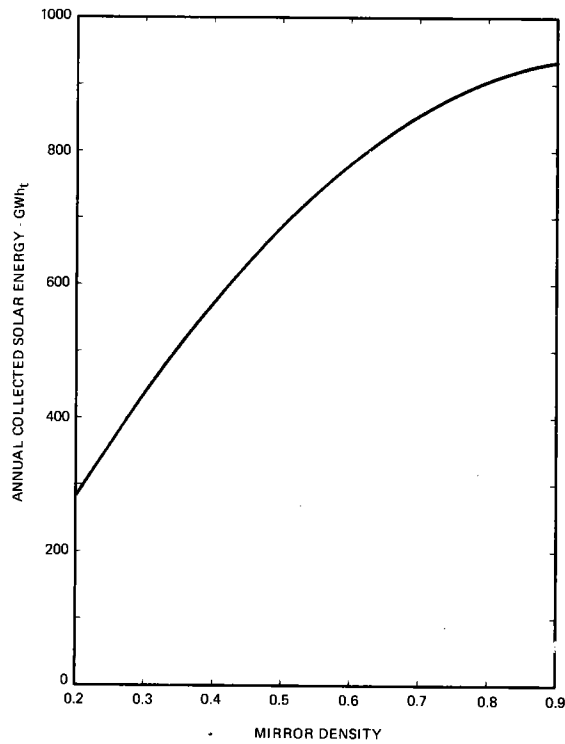


Figure 4. Annual Collected Solar Energy Versus System Mirror Density

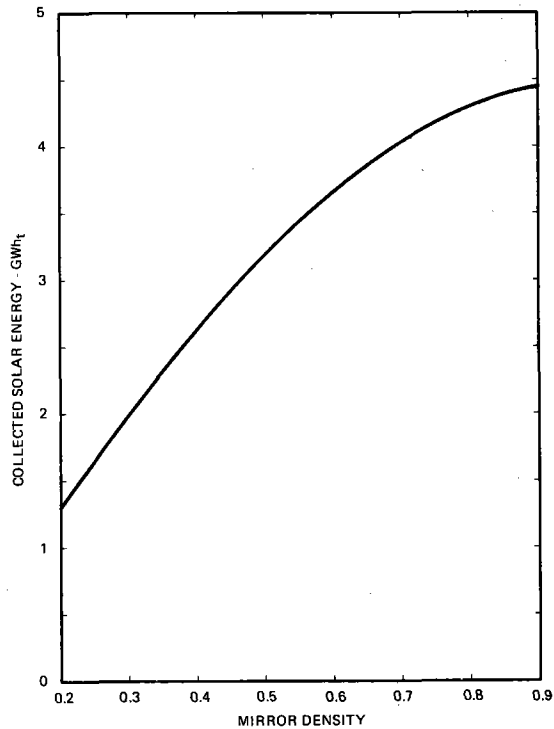


Figure 5. Solar Energy Collected on the Summer Solstice Versus System Mirror Density

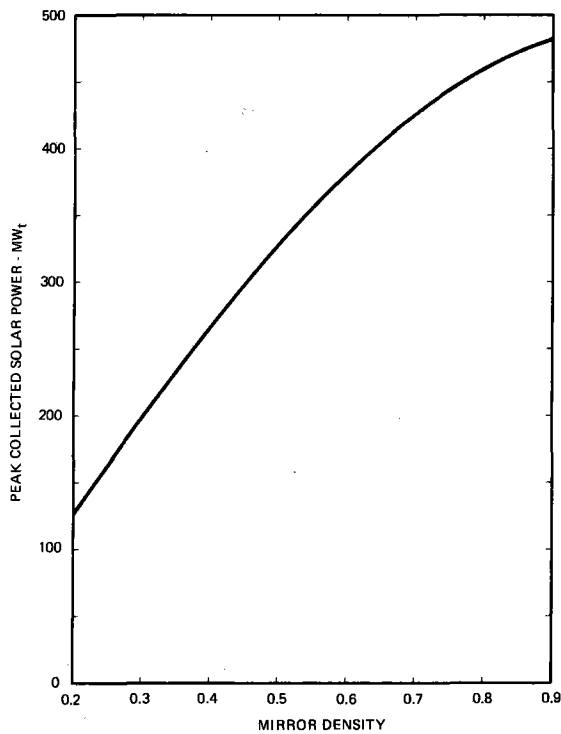


Figure 6. Peak Solar Power Collected on the Summer Solstice Versus System Mirror Density

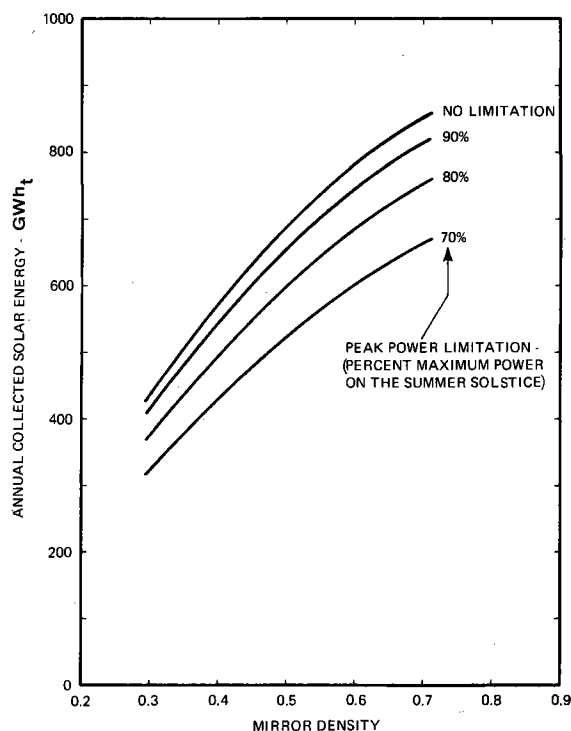


Figure 7. Annual Collected Solar Energy Versus Mirror Density for Peak Power Limitations of 90, 80, and 70 Percent of the Maximum Available Power on the Summer Solstice

The solar energy collected annually by the nominal system over a range of mirror densities is given in Figure 8 for the nominal value of aperture area and for aperture areas of 2, 3, and 4 times the nominal area. This data illustrates the effect of increasing aperture area to allow for greater mirror aiming and focusing errors while still admitting all the reflected energy into the cavity interior. It is assumed that all the cavity dimensions vary as the square root of the aperture area. At a mirror density of 0.5, increasing the aperture area by a factor of four (and doubling cavity dimensions) changes the annual collected solar energy from 687 GWh_t to 611 GWh_t, a decrease of 11 percent. Accompanying the energy decrease would be a cost increase for the larger size cavity receiver and a stronger supporting tower.

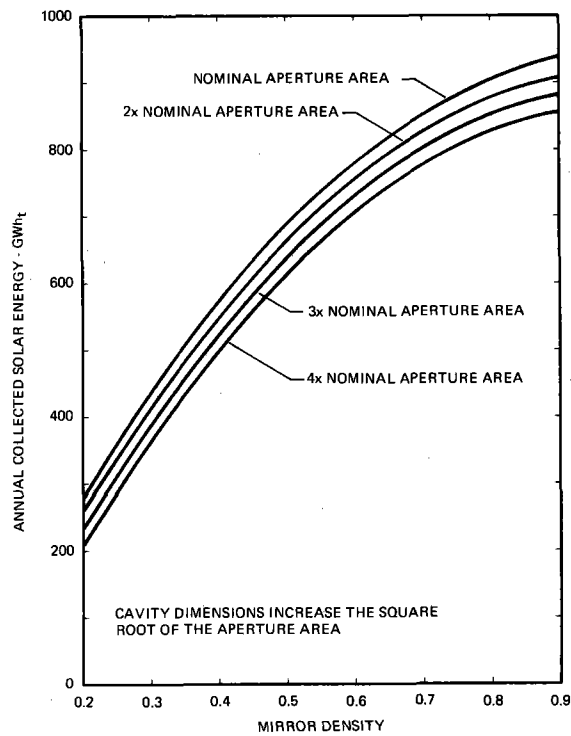


Figure 8. Annual Collected Solar Energy Versus Mirror Density for Various Cavity Aperture Areas

APPENDIX A--CALCULATING THE DIRECTION OF THE SUN

The calculation of solar flux reflected from a mirror at a point in a mirror field requires the direction of the sun from the system site. This "sun" vector is given as a unit vector in the system site reference frame as:

$$\begin{aligned}\vec{s} = & \vec{i} [\sin \phi \sin \alpha \sin \beta - \cos \phi (\cos \delta \cos \beta + \cos \alpha \sin \delta \sin \beta)] \\ & + \vec{j} [\sin \delta \cos \beta - \cos \alpha \cos \delta \sin \beta] \\ & + \vec{k} [\sin \phi (\cos \delta \cos \beta + \cos \alpha \sin \delta \sin \beta) + \cos \phi \sin \alpha \sin \beta]\end{aligned}$$

where

\vec{s} is a unit vector in the system site reference frame pointing toward the sun.

$\vec{i}, \vec{j}, \vec{k}$ are a set of mutually perpendicular unit vectors in the system site reference frame pointing upward, East, and North respectively.

β is the "day" angle, and represents the day of the year when the earth is in a particular position in its orbit (assumed to be circular) around the sun. On the autumn equinox β is equal to zero or 2π .

α is the axis tilt of the earth. (23.45°)

ϕ is the latitude of the system site.

δ is the "hour" angle which represents the earth's rotation about its own axis.

The value of β is assumed to be constant over a day, when, in reality, β increases on the average of about 1/2 degree between dawn and sunset.

Values of α , β , and ϕ --the tilt of the earth's axis, the day of the year, and the system site latitude--are input and the equation for \vec{s} is

solved for the hour angle δ . The \vec{i} component of the sun vector \vec{s} is zero at sunrise and sunset, so that at these times the hour angle δ can be found from

$$\sin \phi \sin \alpha \sin \beta - \cos \phi \cos \beta \cos \delta - \cos \alpha \sin \beta \sin \delta = 0$$

If $C_1 = \cos \phi \cos \beta$, $C_2 = \cos \alpha \sin \beta$, and $C_3 = \sin \phi \sin \alpha \sin \beta$, then

$$C_1 \cos \delta + C_2 \sin \delta = C_3$$

Now divide by $C_1^2 + C_2^2$ and introduce an angle ψ such that

$$\cos \psi = \frac{C_1}{C_1^2 + C_2^2} \quad \text{and} \quad \sin \psi = \frac{C_2}{C_1^2 + C_2^2}$$

Then

$$\cos \psi \cos \delta + \sin \psi \sin \delta = \frac{C_3}{C_1^2 + C_2^2}$$

and

$$\cos (\delta - \psi) = \frac{C_3}{C_1^2 + C_2^2}$$

Since δ has two values, one for dawn and one for sunset,

$$\cos (\delta - \psi) = \pm \frac{C_3}{C_1^2 + C_2^2}$$

$$\delta - \psi = \pm \cos^{-1} \frac{C_3}{C_1^2 + C_2^2}$$

Substituting for ψ

$$\delta = \cos^{-1} \frac{C_1}{C_1^2 + C_2^2} \pm \cos^{-1} \frac{C_3}{C_1^2 + C_2^2}$$

$$\delta = \delta_n \pm \delta_{ds}$$

The first term δ_n is the solution for the noon hour angle and the second term $\pm \delta_{ds}$ provides the hour angle from noon to dawn or to sunset.

The value of δ for the desired day and time is computed ($\delta \pm 15^\circ/\text{hour}$ from solar noon) and values of α , β , ϕ , and δ are used to calculate the sun vector \vec{s} in terms of \vec{i} , \vec{j} , and \vec{k} .

APPENDIX B--CALCULATING INCIDENT SOLAR FLUX

The incident solar flux transmitted directly through the atmosphere is required for the calculation of solar flux reflected from a point-focus mirror field. In addition, the diffuse solar flux from the sky and clouds is also needed when the calculated total solar flux is required to match the measured total solar flux.

Direct solar flux is calculated as:

$$I_D = ST^m \quad (B-1)$$

and

$$I_{Dh} = I_D \cos \gamma = ST^m \cos \gamma \quad (B-2)$$

where

I_D is the direct solar flux transmitted through the atmosphere incident on a plane perpendicular to the sun's rays.

I_{Dh} is the direct solar flux incident on a horizontal surface

S is the solar constant--the extraterrestrial solar flux

T is the atmospheric transmissivity

m is the air mass ratio--the ratio of the mass of air on the path of the transmitted solar flux to the mass of air on a vertical path through the atmosphere

γ is the angle between the vertical and the sun direction

Because the earth travels around the sun in an elliptical orbit, the solar constant S varies about ± 3 percent during the year. The apparent solar constant used for calculations of transmitted direct solar flux on clear days is shown in Figure B-1.

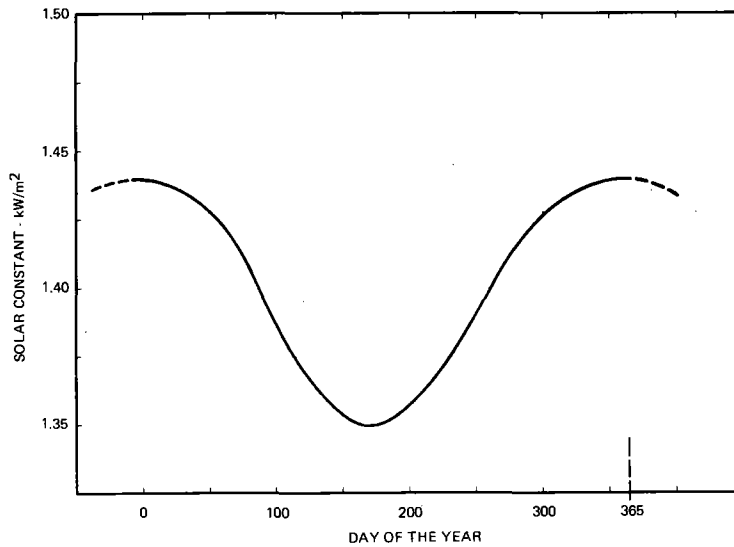


Figure B-1. Apparent Solar Constant Versus the Day of the Year

The apparent solar constant and the apparent atmospheric transmissivity T , as shown in Figure B-2, were determined from climatological data from the U. S. Department of Commerce for Albuquerque, New Mexico. Atmospheric turbidity (humidity, dust, smog, etc.) was not treated explicitly but was included in the variations in atmospheric transmissivity. The air mass ratio m was calculated using data for a 1962 U. S. Standard Atmosphere. The commonly used relationship of $m = 1/\cos \gamma$, where γ is the angle of the sun direction from the vertical, was not used since the assumed system site at Albuquerque, New Mexico, is at an altitude of 1620 meters.

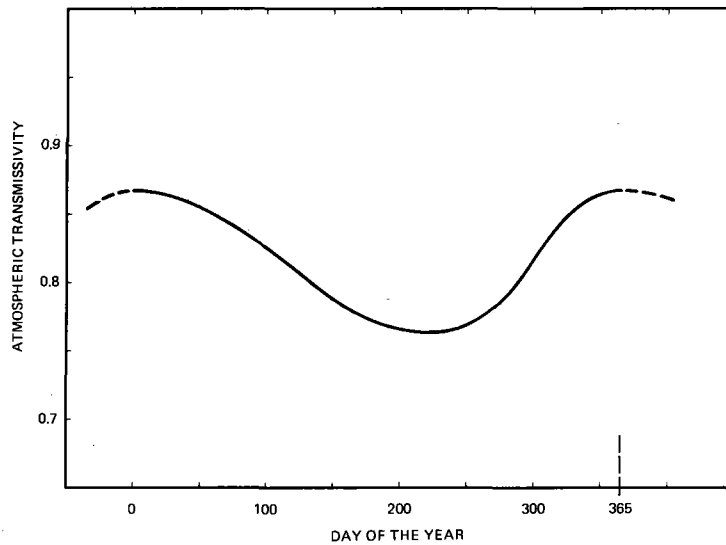


Figure B-2. Apparent Atmospheric Transmissivity for a Clear Day Versus the Day of the Year

Diffuse solar radiation from sky and clouds is calculated using the following relationships developed by Liu and Jordan.³ First, the monthly average daily diffuse radiation is found from the monthly average daily total variation by the relationship:

$$\bar{D} = 0.797 \bar{H} - 0.8364 \bar{H}^2 / H_{oh} \quad (B-3)$$

where

\bar{D} is the monthly average daily diffuse radiation on a horizontal surface

\bar{H} is the monthly average daily total radiation on a horizontal surface

H_{oh} is the extraterrestrial daily total radiation on a horizontal surface

The diffuse solar flux for a cloudy sky is then found by the following relationship given by Liu and Jordan:

$$I_{dh} = \bar{D} r_d = \bar{D} \frac{\pi}{24} \left(\frac{\cos \omega - \cos \omega_s}{\sin \omega_s - \omega_s \cos \omega_s} \right) \quad (B-4)$$

where

I_{dh} is the diffuse solar flux (for a hazy or cloudy sky) on a horizontal surface at the time of day represented by the hour angle ω

\bar{D} is the monthly average daily diffuse radiation on a horizontal surface

r_d is the diffuse flux factor

ω is the hour angle of the time of interest

ω_s is the sunset hour angle

This calculation of diffuse flux on a hazy or cloudy day, combined with the direct flux calculation, gives results that are in good agreement with the relationship of direct solar flux to the percentage of possible total solar flux developed by the Aerospace Corporation.

The diffuse solar flux for a clear day is given by the following Liu and Jordan relationship:

$$I_{dh} = 0.271 I_{oh} - 0.2939 I_{Dh} \quad (B-5)$$

where

I_{dh} is the diffuse solar flux as defined above

I_{oh} is the extraterrestrial solar flux on a horizontal surface

I_{Dh} is the direct solar flux on a horizontal surface

The total daily solar radiation incident on a surface is found by summing the direct and diffuse solar flux at intervals (twenty minutes in this study) throughout the day and multiplying the summed flux by the time interval. An annual system performance model was developed by modeling each month as an average day and then summing the performance of each average day times the number of days it represents. The effects of local weather are modeled by adjusting the solar constant for each average day such that the calculated daily total solar radiation on a horizontal surface agrees with the monthly average daily total solar radiation given for a particular locale in the U. S. Climatic Atlas. The adjusted solar constant S is used for calculating the transmitted direct solar flux, while the solar constant S' used for calculating the extraterrestrial daily total radiation remains unchanged.

The desired value of total daily radiation on a flat surface (from the Climatic Atlas or elsewhere) divided by the time interval between calculations throughout the day gives the desired value of direct and diffuse solar flux summed over the day, expressed as follows:

$$\bar{H}/t = \Sigma I_{Th} = \Sigma(I_{Dh} + I_{dh}) = \Sigma I_{Dh} + \Sigma I_{dh} \quad (B-6)$$

where t is the integration time step between flux calculations. Now substituting I_{Dh} and I_{dh} from Equations (B-1) and (B-2) gives

$$\bar{H}/t = \Sigma S T^m \cos \gamma + \Sigma (0.797\bar{H} - 0.836 \bar{H}^2 / H_{oh}) r_d \quad (B-7)$$

Substituting

$$H_{oh} = t \Sigma S' \cos \gamma,$$

$$\bar{H}/t = \Sigma S T^m \cos \gamma + \Sigma [0.797\bar{H} - 0.836 \bar{H}^2 / (t \Sigma S' \cos \gamma)] r_d \quad (B-8)$$

Now, moving the constants outside the summation signs and solving for S gives

$$S = \bar{H}/t - [0.797 \bar{H} - 0.836 \bar{H}^2 / (tS' \Sigma \cos \gamma)] \Sigma r_d / (\Sigma T^m \cos \gamma) \quad (B-9)$$

This is the expression for the adjusted value of S that, when used to calculate the transmitted direct solar flux and combined with the calculated diffuse solar flux, yields a daily total solar flux equal to the desired value from the Climatic Atlas.

APPENDIX C--DETERMINING REFLECTED SOLAR FLUX

The total solar power reflected to the cavity receiver is found by dividing the mirror field into sections and summing the reflected solar power from all the sections to obtain the system total. The sections of the mirror field are laid out on a square grid and then the circular mirror field boundary is used to eliminate those sections outside the mirror field radius and to reduce the area of those sections cut by the mirror field boundary. The reflected solar power--diminished by shadowing of incident flux and blocking of reflected flux by adjacent mirrors--is found for a unit area of mirror at the center of a section. This value is then multiplied by the mirror density (mirror area/ground area) and the section area to give the total solar power reflected by that section. This method assumes that the mirror conditions at the section center hold over the entire section. Since the results from a 100-section mirror field were within one-half percent of those results obtained from a 400-section mirror field, a 100-section mirror field was used to reduce computer time.

The reflected solar power for a unit area of mirror at the center of a section is found by calculating the solar power reflected by an individual round mirror at the section center--including effects of shadowing and blocking--and dividing by the area of that mirror. For calculating the effects of shadowing and blocking, the center mirror is modeled as being in the center of a hexagonal pattern surrounded by the six nearest mirrors and the six next nearest mirrors. The orientation of the center mirror is determined by defining the unit normal vector at the mirror center as the unit vector which bisects the angle between the sun direction vector and the reflection vector from the center of the mirror to the center of the cavity receiver aperture. The assumption is made that the adjacent mirrors which do the shadowing and blocking in the hexagonal mirror pattern have their unit normal vectors pointed in the same direction as the center mirror. Actually, the adjacent mirrors are not quite parallel. However, the slight differences in mirror directions have a negligible effect on the calculations.

Because the center mirror and all adjacent mirrors are essentially parallel, an adjacent mirror which shadows the center mirror casts a shadow on the center mirror which is a section of a circle having the same radius as the round mirrors. In a like way, the blocking of reflected solar flux by an adjacent mirror can be projected backward onto the center mirror as a circular section. Thus, the area of the center mirror can be divided

into an effective area which reflects solar flux to the cavity receiver and an ineffective area (bounded by a perimeter made up of circular arcs) which is either shadowed or blocked by adjacent mirrors. The ratio of effective area to total area of a mirror is a function of mirror density and is independent of mirror size.

The reflected solar power is calculated for the effective reflecting area of the center mirror and divided by the total area of the center mirror to give the reflected solar power per unit area of mirror at that time of day and for that mirror location. This power per unit area is then multiplied by the mirror density and section area to give the total solar power reflected toward the cavity receiver from the section at that given time. Summing the results of similar calculations for each section gives the solar power reflected from the entire field toward the cavity receiver at that time. This solar power is then multiplied by the time interval between calculation steps to give the amount of solar energy reflected during the interval.

The solar power entering the cavity aperture is assumed to be four percent less than the power reflected by the mirror field to account for blocking by the supports which hold the cavity receiver at the top of the tower.

REFERENCES

1. Brumleve, T. D., A High Temperature Solar Energy System, SLL-73-0059, Sandia Laboratories, August 1973.
2. Gamier, B. J., and Ohmura, A., The Evaluation of Surface Variations in Solar Radiation Income, Solar Energy, Vol. 13, No. 1, pp. 21-24, April 1970.
3. Liu, B. Y. H., and Jordan, R. C., The Interrelationship and Characteristic Distribution of Direct, Diffuse, and Total Solar Radiation, Solar Energy, Vol. 4, No. 3, July 1960.
4. Solar Thermal Conversion Mission Analysis, Vol. III, Southern California Insolation Climatology, The Aerospace Corporation, Report No. ATR-74 (7417-05)-1, January 15, 1974.
5. U. S. Standard Atmosphere, 1962 prepared under the sponsorship of the National Aeronautics and Space Administration, the United States Air Force and the United States Weather Bureau, December 1962.
6. Skinrood, A. C., Brumleve, T. D., Schafer, C. T., Yokomizo, C. T., Leonard, C. M., Status Report on a High Temperature Solar Energy System, SAND74-8017, September 1974.
7. Climatological Data, National Summary, 1970 through 1973, U. S. Department of Commerce, National Oceanic and Atmospheric Administration, Environmental Data Service.

UNLIMITED RELEASE

INITIAL DISTRIBUTION:

Dr. Edward H. Fleming, Jr.
Maj. Gen. Ernest Graves
Dr. Jack Vanderryn
Dr. James C. Bresee
Mr. James E. Rannels (10)
U. S. Atomic Energy Commission
Washington, D. C. 20545

Dr. Lloyd O. Herwig
Mr. George Kaplan
National Science Foundation
1800 G. Street
Washington, D. C. 20550

Dr. D. E. Anderson
Mr. Ross A. Stickley
Sheldahl, Inc.
Northfield, Minnesota 55057

Mr. Dwain Spencer
Electric Power Research Institute
3412 Hillview Avenue
Palo Alto, California 94304

Mr. Floyd A. Blake
Martin Marietta Aerospace
P. O. Box 179
Denver, Colorado 80122

Mr. John Blewett,
Attn: J. G. Cottingham
Brookhaven National Laboratory
Upton, L. I., New York 11973

Mr. Piet B. Bos
Aerospace Corporation
P. O. Box 92957
Los Angeles, California 90045

Mr. G. W. Braun
Southern California Edison
2244 Walnut Grove Ave.
Rosemead, California 91770

Dr. Jesse C. Denton
National Center for Mfg. and Power
University of Pennsylvania
Philadelphia, Pennsylvania 19104

Dr. Alvin F. Hildebrandt
Dr. Loren L. Vant Hull
Department of Physics
University of Houston
3801 Cullen Boulevard
Houston, Texas 77004

Mr. Peter Hindley
Mr. John Gumz
Pacific Gas and Electric
77 Beale St.
San Francisco, California

Mr. Sig Hansen
Mr. Les Hill
State of California
Energy Planning Council
1127 L Street
Sacramento, California

Dr. S. Karaki
Department of Civil Engineering
Engineering Research Center
Colorado State University
Fort Collins, Colorado 80521

Mr. Ron Larson
Congress of the United States
Office of Technology Assessment
Washington, D. C. 20501

Dr. George Löf
158 Fillmore Street
Suite 204
Denver, Colorado 80206

Mr. John Martin
Argonne National Laboratory
Argonne, Illinois 60439

Mr. Jerry Powell
Mr. R. N. Schmidt
Honeywell Systems and Research Center
2600 Ridgeway Parkway
Minneapolis, Minnesota 55413

M. Sparks, 1
W. J. Howard, 2
C. Winter, 4010
D. B. Shuster, 4700
A. Narath, 5000
J. H. Scott, 5700
G. E. Brandvold, 5710
R. H. Braasch, 5712
R. P. Stromberg, 5717
T. B. Cook, Jr., 8000
L. Gutierrez, 8100
C. S. Selvage, 8180
R. J. Tockey, 8181
D. N. Tanner, 8182
R. I. Peterson, 8183
A. C. Skinrood, 8184 (20)
T. D. Brumleve, 8184
C. M. Potthoff, 8185
C. H. DeSelm, 8200
B. F. Murphey, 8300
T. S. Gold, 8320; Attn: R. L. Rinne, 8321
J. D. Hankins, 8322
J. F. Barham, 8360; Attn: R. C. Wayne, 8365
C. M. Leonard, Jr., 8365 (2)
W. C. Scrivner, 8400
G. C. Newlin, 6011 (3)
Technical Publications and Art Division, 8265, for TIC (2)
F. J. Cupps, 8265/Classification and Technical Library
Processing Division, 3141
Classification and Technical Library Processing Division, 3141 (4)
Library and Security Classification Division, 8266-2 (5)